Supporting Information

Atomic-level ablation of Au@Ag NRs using ultrafast laser

Dezhi Zhu, Jianfeng Yan*, Jiawang Xie, Guangzhi He

State Key Laboratory of Tribology, Department of Mechanical Engineering, Tsinghua University, Beijing 100084, China.

* Corresponding author. Email: yanjianfeng@tsinghua.edu.cn

Finite-Difference Time-Domain (FDTD) simulations (Lumerical Solutions) were conducted to calculate the near-field and far-field properties of the metallic nanoparticles. Geometric parameters of the Au, Au@Ag and Ag nanorods (NRs) were extracted from TEM images. The Au core and Ag shell were modeled as round-ended cylinders of 42 nm × 12 nm and 50 nm × 20 nm, respectively. Calculations were conducted for a single nanoparticle on the carbon film with a thickness of 4 nm. Dielectric permittivities tabulated by Johnson and Christy[1] were used for Au and Ag. To investigate the structural transformation induced by the light irradiation, the geometry of the Au@Ag NRs was modified from a rod shape to either an ellipsoid (end facet tailoring) or a dumbbell (lateral facet tailoring). Calculations of extinction cross-sections were performed for an isolated nanostructure, which was excited at linearly polarized light. The total extinction cross-section was the average of longitudinal and transverse excitations. The distributions of enhanced electric fields were calculated at resonance bands for a parallel polarization. A uniform mesh-grid of 1 nm was used to ensure small structural details and good numerical convergence.

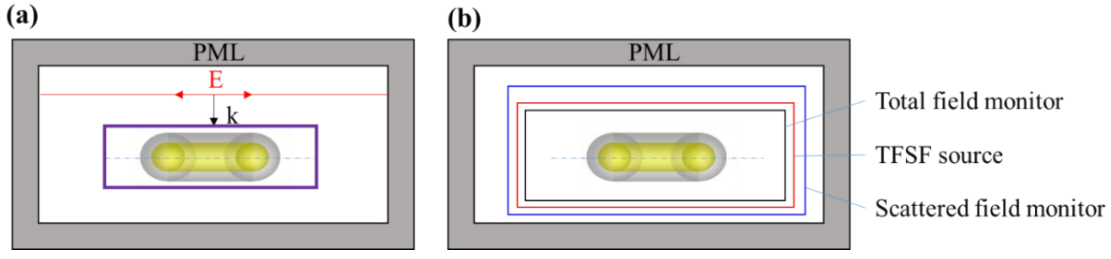

Figure S1. Schematic representation of the geometry used for FDTD calculations. (a) The nanorod was surrounded by a field profile monitor (purple line), to calculate the electric field distribution. The simulation was performed in the direction (black) and polarization (red) of light. (b) The monitors, source, and boundary conditions used in the calculation of extinction cross-sections.

FEM is used to obtain the electromagnetic field and energy deposition of the Au@Ag NR. The electromagnetic analysis is performed by solving Maxwell's equations:

$$\nabla \times \mathbf{H} = \mathbf{J} + \frac{\partial \mathbf{D}}{\partial t} \tag{1}$$

$$\nabla \times \mathbf{E} = -\frac{\partial \mathbf{B}}{\partial t} \tag{2}$$

$$\nabla \cdot \mathbf{D} = \rho \tag{3}$$

$$\nabla \cdot \mathbf{B} = 0 \tag{4}$$

where **E** is the electric field intensity; **D** is the electric displacement; **H** is the magnetic field intensity; **B** is the magnetic flux density; **J** is the current density, and ρ is the electric charge density.

To obtain a closed system, the constitutive relations of the material properties must be included. They are given as follows:

$$\mathbf{D}=\varepsilon\mathbf{E} \tag{5}$$

$$\mathbf{B} = \mu\mathbf{H} \tag{6}$$

$$\mathbf{J} = \sigma\mathbf{E} \tag{7}$$

where ε and μ are the permittivity and permeability of the material, respectively; σ is the conductivity of the material.

By solving the Maxwell equations, the local electric field is obtained. The local energy deposition on the Au@Ag NR is given as

$$q = \frac{n_0^2 \omega}{2} \mathrm{Im}(\varepsilon) |\mathbf{E}|^2 \tag{8}$$

where n_0 is the optical index of the surrounding medium, and ω is the frequency of the laser.

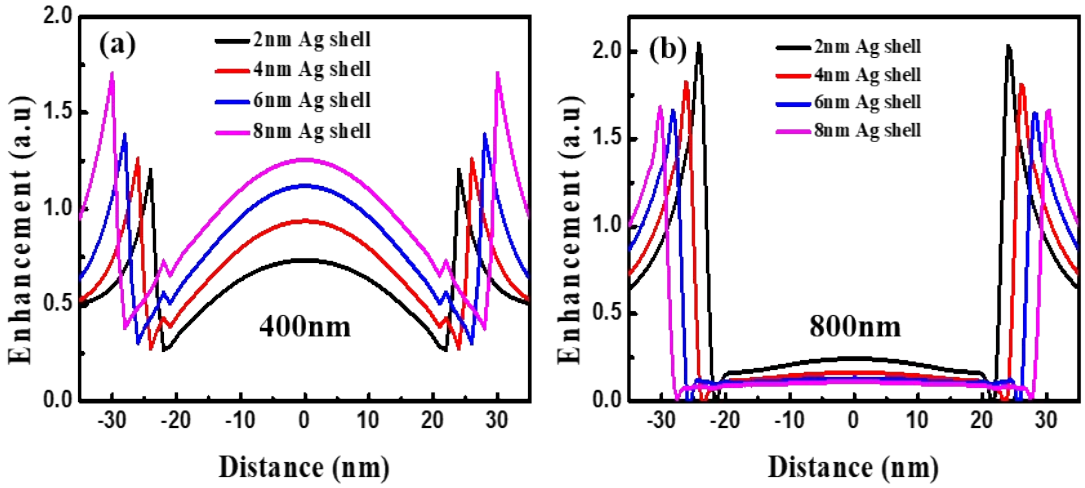

Figure S2. Electric field enhancement profiles along the longitudinal axis of Au@Ag nanorods with Ag shells of different thicknesses at wavelengths of (a) 400 nm and (b) 800 nm.

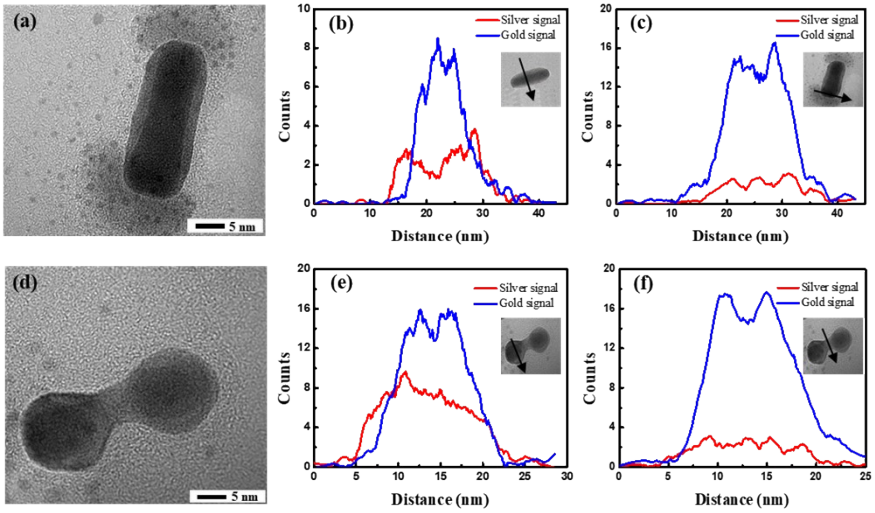

Figure S3. (a) Ellipsoid nanostructure obtained after 800 nm-wavelength pulse irradiation, and the Ag shells at two end are ablated. (b) Elemental distribution of Au and Ag along the transverse axis of 4 nm-Ag shell Au@Ag nanorods indicated by line scanning in the inset. (c) The line scanning at the end of the ellipsoid nanostructure. (d) The dumbbell nanostructure obtained after 400 nm-wavelength pulse irradiation, and the Ag shells in the middle are ablated. The line scanning at (e) the end and (f) middle of the dumbbell nanostructure.

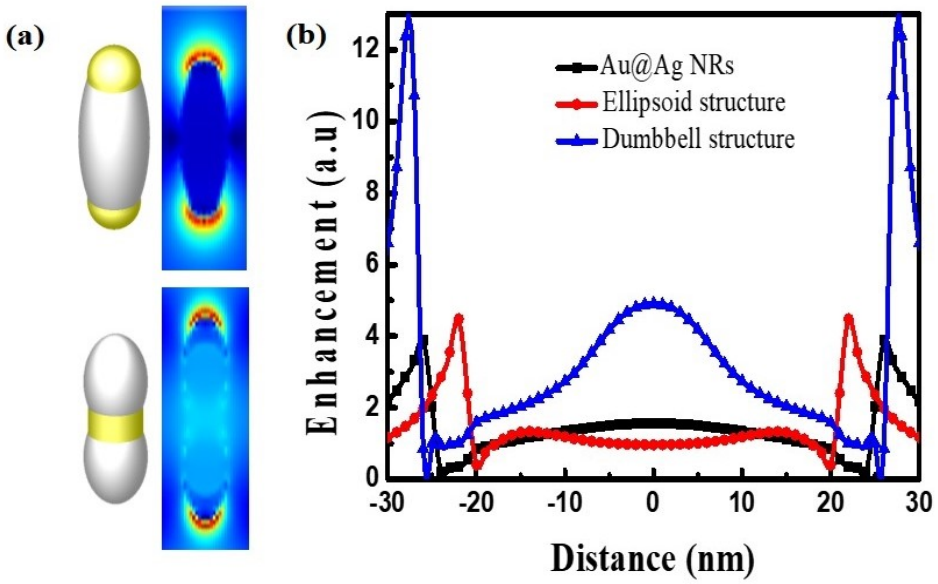

Figure S4. (a) Calculated electric field distribution of ellipsoid and dumbbell nanostructures excited at resonance bands. (b) Calculated electric field enhancement profiles along the longitudinal axis of Au@Ag NRs, ellipsoid, and dumbbell nanostructures.

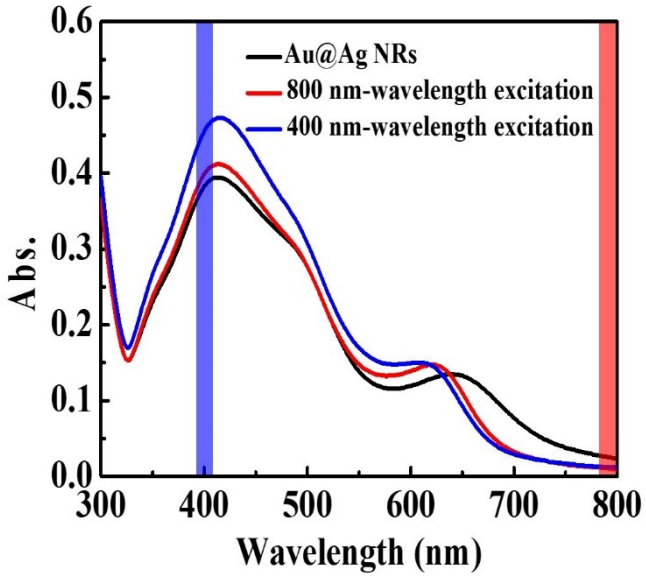

Figure S5. UV-vis absorption spectra of as-prepared Au@Ag NRs and Au@Ag nanostructures after 800 nm- and 400 nm-wavelength femtosecond laser pulse irradiation.

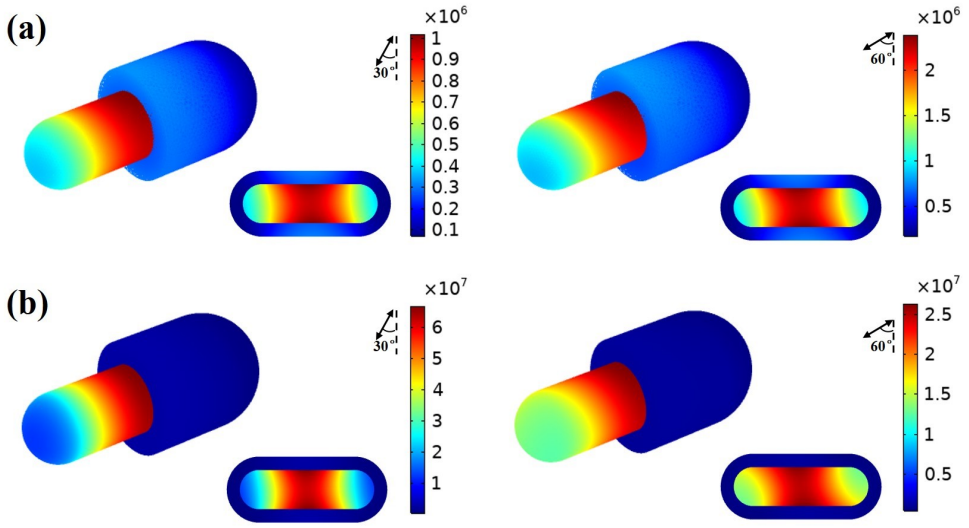

Figure S6. Calculated energy density distribution on Au@Ag NRs excited at (a) 800-nm and (b) 400-nm laser pulse at polarization angles of 30° and 60°.

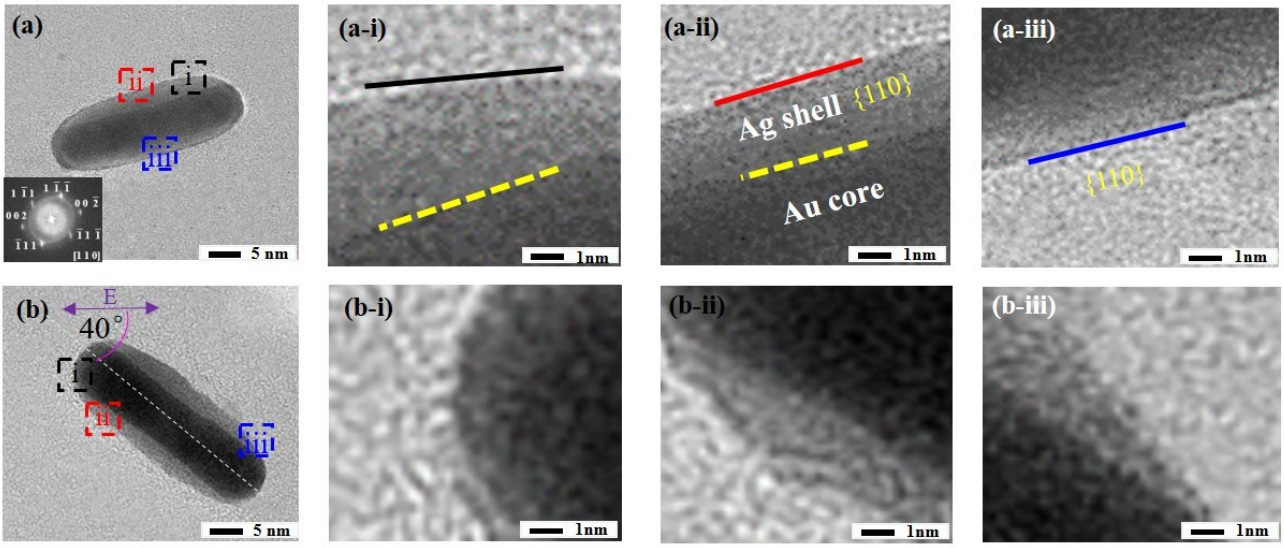

Figure S7. TEM images of the atomic level structures of Au@Ag NRs. (a) As-prepared NRs. (b) The nanostructure obtained after 800 nm-wavelength pulse irradiation with a 40° polarization angle. ((a, b)-i, ii, iii) High resolution TEM images of the atomic arrangements in three various regions. The inset in (a-i) is the fast Fourier transform image. The color lines represent the edge contour of NRs.

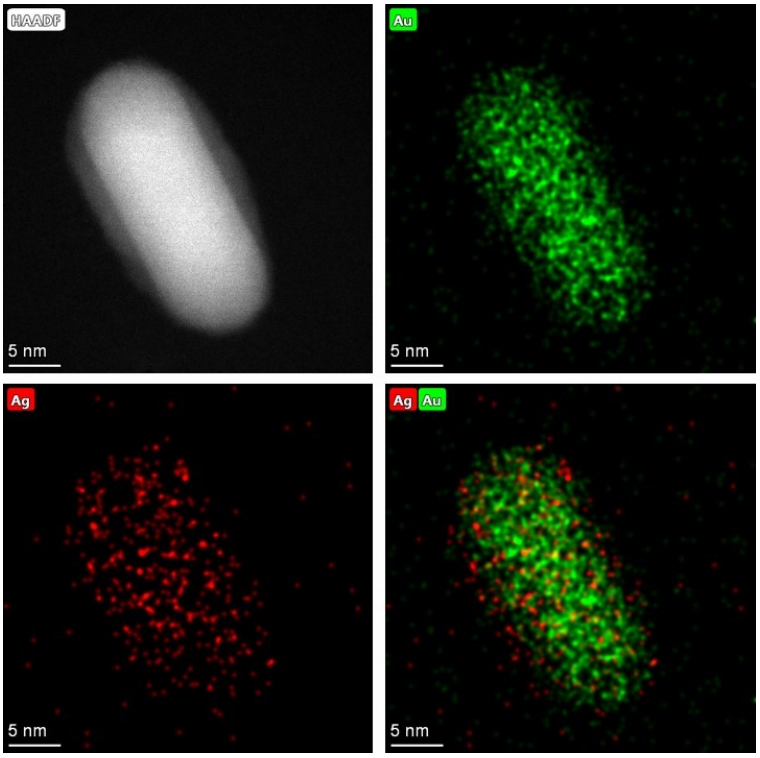

Figure S8. HAADF-STEM images of individual ellipsoid nanostructure after 800 nm-wavelength pulse irradiation with a 60° polarization angle and EDS elemental mapping of Au and Ag.

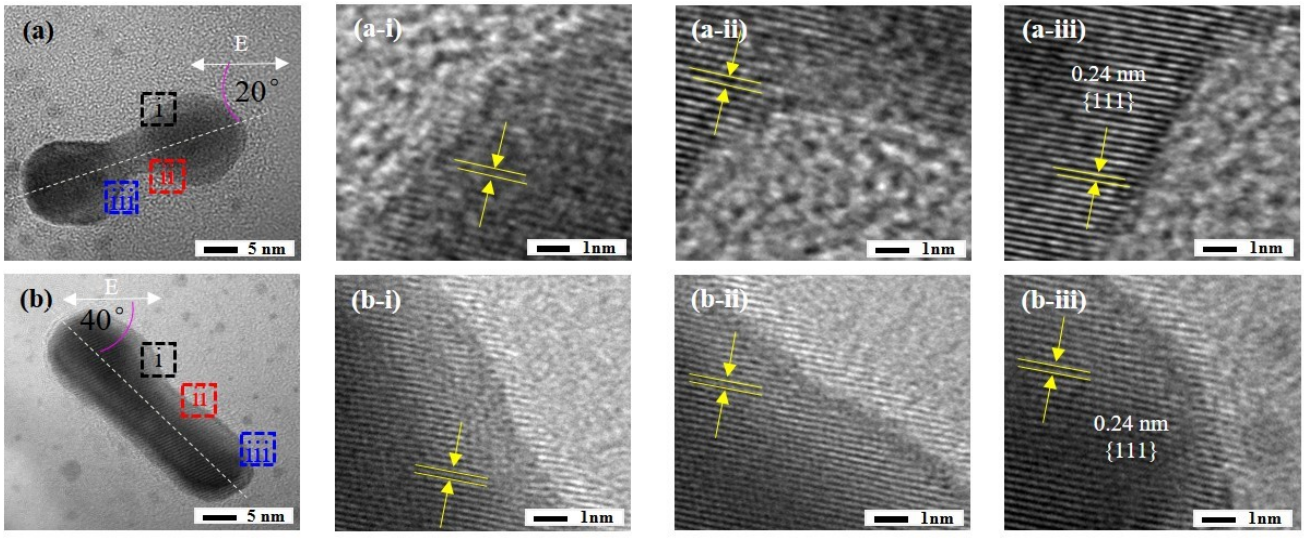

Figure S9. TEM images of the atomic level structures of Au@Ag NRs. (a) The nanostructure obtained after 400 nm-wavelength pulse irradiation with a 20° polarization angle. (b) The nanostructure obtained after 400 nm-wavelength pulse irradiation with a 40° polarization angle. ((a, b)-i, ii, iii) High resolution TEM images of the atomic arrangements in three various regions.

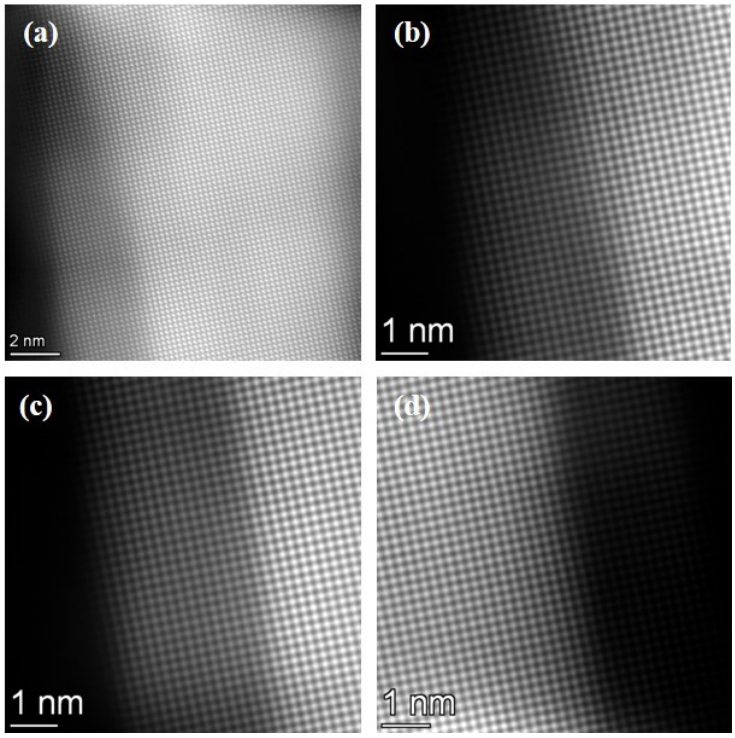

Figure S10. HAADF-STEM images of the atomic-level structure of irradiated metallic NRs.

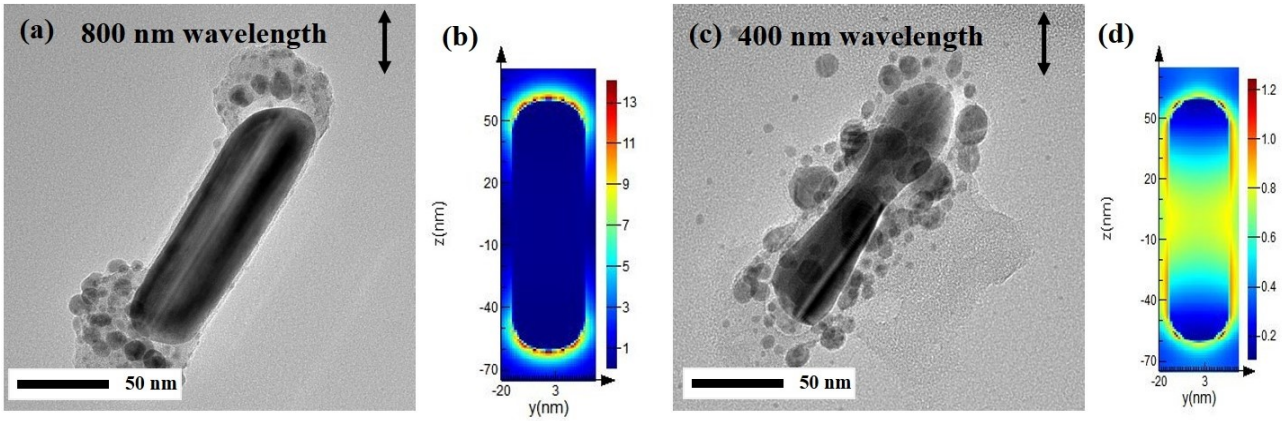

Figure S11. TEM images and corresponding calculated electric field distributions of Ag NRs after irradiation with (a, b) parallel polarization and 800 nm-wavelength pulse, and (c, d) parallel polarization and 400 nm-wavelength pulse. Ag NRs were synthesized using a previously reported protocol[2] with slight modifications.

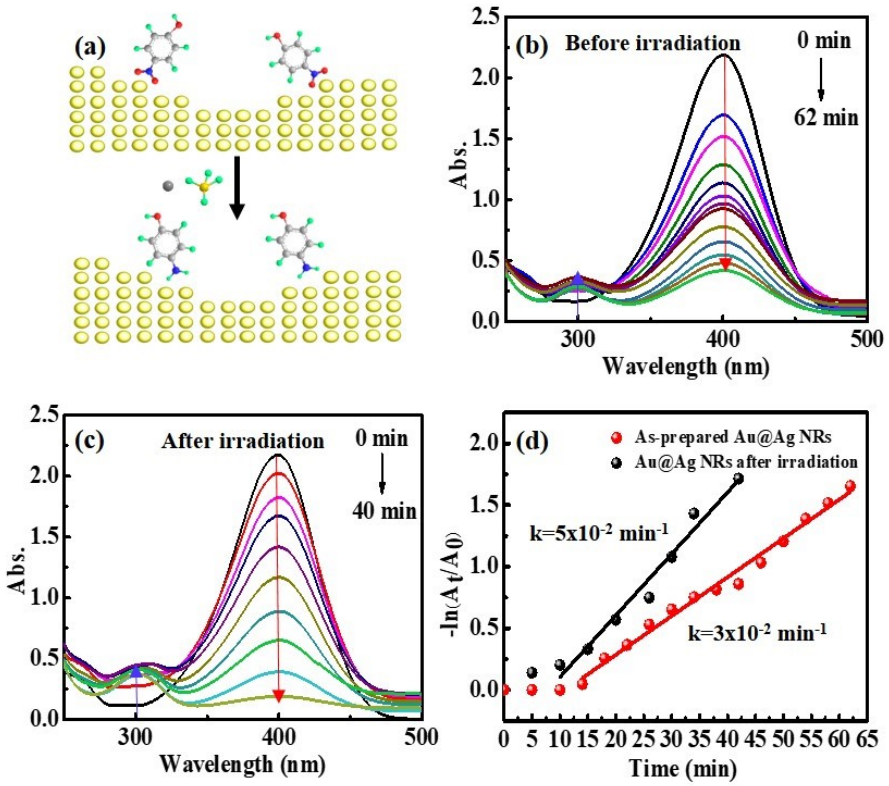

Figure S12. (a) Schematic illustration of the reduction reaction of surface-adsorbed 4-NP to 4-AP catalyzed by the NRs with atomic steps. Time-dependent UV-vis absorption spectra in the presence of (b) as-prepared Au@Ag NRs and (c) Au@Ag nanostructures after 800 nm-wavelength femtosecond laser pulse irradiation. (d) The dependence of $-\ln(A_t/A_0)$ on time for Au@Ag nanostructures.

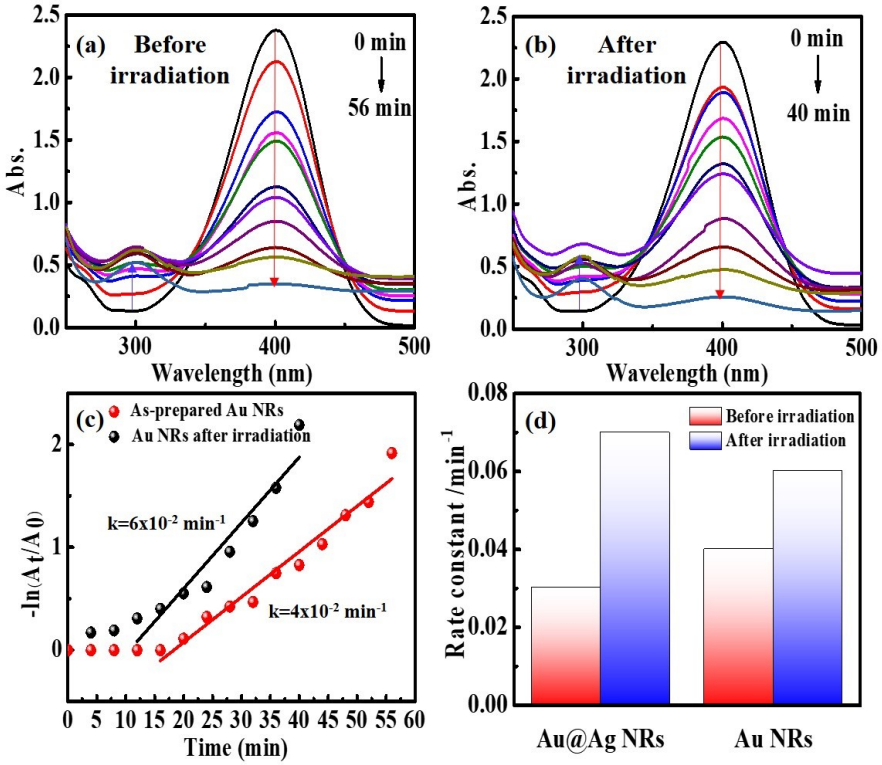

Figure S13. Time-dependent UV-vis absorption spectra of 4-NP by $NaBH_4$ in the presence of (a) as-prepared Au NRs and (b) Au nanostructures after 400 nm-wavelength femtosecond laser pulse irradiation. (c) The dependence of $-\ln (A_t/A_0)$ on time for the reduction of 4-NP in the presence of Au nanostructures. (d) The rate constants of the surface reactions on Au@Ag and Au nanostructures.

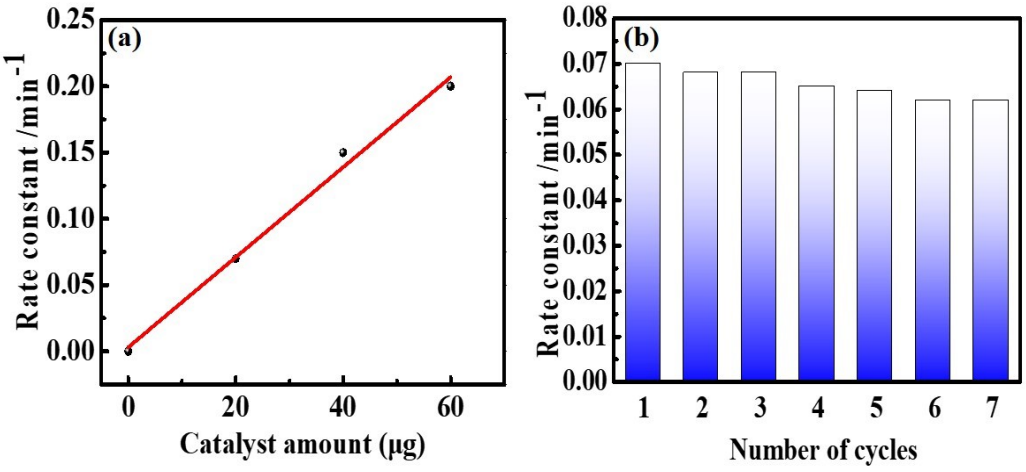

Figure S14. (a) Plot of the rate constants versus irradiated Au@Ag NRs amount. (b) Plots of the rate constants versus the number of successive cycles (irradiated Au@Ag NRs).

References

1 Johnson, P. B. and Christy, R. W., *Phys. Rev. B: Condens. Matter*, 1972, **6**, 4370-4379.

2 Hu, J. Q., Chen, Q., Xie, Z. X., Han, G. B., Wang, R. H., Ren, B., Zhang, Y., Yang, Z. L. and Tian, Z. Q., *Advanced Functional Materials*, 2010, **14**, 183-189.